RSC Advances

ROYAL SOCIETY OF CHEMISTRY

www.rsc.org/advances

Photofragment Ionization-loss Stimulated Raman Spectroscopy of a Hydrated Neurotransmitter: 2-Phenylethylamine–water

Nitzan Mayorkas, Snir Cohen, Hanan Sachs and Ilana Bar*

Different types of spectral signatures and their interpretation provide valuable information on intra- and inter-molecular interactions that lead to unique shapes of molecules and clusters. Here, ionization-loss stimulated Raman (ILSR) spectra of the 2-phenylethylamine-water (PEA-H_2O) cluster were obtained by monitoring the spectral signatures of PEA and of CH_2NH_2-H_2O (a hydrated portion of the PEA tail) fragment ions. The ILSR spectra of both fragments were found to be similar, indicating that they are actually reminiscent of the PEA-H_2O cluster signature. Comparison of the photofragment spectra to anharmonic calculated Raman spectra of the different conformers of the PEA-H_2O clusters, suggests a structure with PEA similar to that of the most stable gauche conformer, with H_2O hydrogen bonded to the nitrogen lone pair.

submitted to RSC Adv.

Department of Physics, Ben-Gurion University of the Negev, Beer-Sheva 84105, Israel

E-mail: ibar@bgu.ac.il.

† Electronic supplementary information (ESI) available. See DOI:

1 Introduction

The investigation of the spatial arrangements of biomolecules and of the forces that lead to them is usually adopted as a reductionist approach[1] towards eventual understanding of molecular processes playing a central role in biospecific recognition. In principle, the structures of isolated molecules are a result of intra-molecular interactions and in other environments a consequence of a delicate balance between intra- and inter-molecular interactions. Therefore, obtaining information regarding these interactions is of particular importance for getting insight into the structures and intrinsic molecular properties of isolated biomolecular building blocks and their clusters.[2,3,4,5,6,7,8,9]

Structures are usually revealed by comparing the spectroscopic results for molecules or their clusters in the gas phase, to high level quantum calculations. Indeed, a variety of experimental techniques, including electronic, vibrational and rotational spectroscopies combined with results of quantum calculations are employed to assess detailed structural pictures of the conformational landscapes of biomolecules.

A molecule that attracted considerable interest is the 2-phenylethylamine (C_6H_5–CH_2–CH_2–NH_2, PEA) that contains a rigid skeleton ring and a flexible ethylamino side chain.[10,11,12,13,14,15,16,17,18] This model system reflects the parent structure of a group of amine compounds functioning in biological systems as neurotransmitters and neuromodulators and was observed to fold into several different conformers in the gas phase. Different methods revealed the presence of four,[10] two,[16] and five conformers,[11] where the fifth one[13] was reassigned to a water cluster. Eventually, the presence of four conformers was confirmed by additional experimental investigations combined with the results of quantum calculations.[12,14,15,17,18]

These studies revealed that the flexibility of the ethylamine side chain in PEA, which is a consequence of the two principal flexible coordinates, including internal rotation about the C_α-C_β and C_α-N single bonds, affords the existence of the conformers. In particular it has been found that the two lowest and two highest energy conformers of PEA correspond to structures with the ethylamino side chain folded (gauche) and extended (anti). In the gauche conformers, the amino hydrogen atoms are oriented differently toward the aromatic ring to form unique weakly N–H$\cdots\pi$ hydrogen bonded (HB) structures, slightly stabilizing the isolated molecules. On the other hand, in the anti conformers, the amino hydrogen atoms with symmetric and nonsymmetric orientations, point far away from the ring, leading to less stable conformers, due to HB absence.

The PEA-water clusters were only scantily studied, using laser induced fluorescence excitation and one- and two-color mass-selected resonant two-photon ionization (R2PI) of the $S_1 \leftarrow S_0$ electronic transition, the $M(H_2O)_n$ (n = 1 – 4) clusters were detected.[13,14] Their stoichiometry was assigned on the basis of the observed ion fragmentation patterns, band contour analysis and calculated energy differences between the conformers. Very recently,[19] the rotational spectrum of the most stable PEA-H_2O molecular adduct was studied by free jet absorption microwave spectroscopy.

Nevertheless, vibrational spectral signatures of the PEA-H_2O clusters were not measured yet. In the present work ionization-loss stimulated Raman spectroscopy (ILSRS),[18,20,21,22] where the depletion of ground state species by SR excitation is probed by R2PI, was used. However, in contrast to our previous studies that measured the spectra of different parent ions, here we were interested in testing whether it would be possible to reveal the structure of the PEA-H_2O cluster by photofragment ILSR

spectroscopy. Hence, the ILSR spectra of the fragment ions, i.e., PEA and CH_2NH_2-H_2O (the hydrated portion of the PEA tail) were measured, enabling to infer the characteristic vibrational modes of the PEA-H_2O parent cluster in an extended spectral range. The acquired spectra were compared to the calculated anharmonic Raman spectra of the PEA-H_2O cluster, obtained by density functional theory (DFT) calculations. The structure of the PEA-H_2O cluster could be determined by choosing the calculated spectrum that showed the best overall agreement with the measured photofragment ILSR spectra.

2 Methods

a) Experimental

A pumped Wiley–McLaren home built time-of-flight mass spectrometer (TOFMS), resembling the design of Ref. 23, was used. The TOFMS consists of differentially pumped source and main detection chambers, separated by a skimmer with a 2.0 mm diameter (dia.) aperture. PEA-H_2O clusters were formed by passing a stream of argon, saturated with water, at a pressure of about 1 bar, through the vapor of a PEA sample, purchased from Sigma-Aldrich (99 % pure), held in a reservoir at room temperature. The gas mixture was then expanded through a pulsed nozzle valve (General Valve, Series 9, 0.8 mm orifice) operating at 10 Hz and then through the skimmer before entrance into the main vacuum chamber. The generated molecular beam was introduced into the main chamber, while pointing toward the detection plane and passing through the hole of the repeller.

In the interaction region of the TOFMS, the molecular beam was intersected by the laser beams, allowing measurement of mass-selected R2PI and ILSR spectra. R2PI

spectra were measured using a tunable frequency-doubled pulsed neodymium:yttrium aluminum-garnet (Nd:YAG)-pumped dye laser (UV) with ~ 5 ns pulses at a 10 Hz frequency. For monitoring ILSR spectra, an additional Nd:YAG laser system was employed to provide the SRS beams, while parking the UV laser on resonances, corresponding to the particular species. The additional laser provided the second harmonic (532 nm) with ~ 5 ns pulses at 10 Hz, which was split in a one to four ratio, so that the former supplied the pump beam, ω_p, and the latter pumped a dye laser to generate a tunable ω_S beam. The vertically polarized ω_p and ω_S beams, with energies of ~ 17 mJ and 25 mJ, respectively, were counterpropagated and used to induce the Raman transitions. The ω_p and ω_S beams were focused with 35 and 30 cm focal length (f.l.) planoconvex lenses and aligned to spatially and temporally overlap in the interaction region of the TOFMS. These beams also overlapped the UV beam, focused by the 35 cm f.l. lens, and preceded the UV beam by ~ 30 ns.

Ions obtained via R2PI and ILSR were detected by a micro-channel plate (MCP) and fed into a fast preamplifier, allowing measurement of mass spectra with a fast digital oscilloscope and recording of the integrated intensity of the ion peak of interest. The spectra were monitored by measuring the integrated ion signal as a function of the UV or ω_S beam wavelengths. For each of the species, three to eight spectra were measured and averaged to achieve suitable signal-to-noise levels.

b) Calculations

Quantum mechanical DFT calculations and data treatment were performed, according to our approach in Ref. 22, to aid in interpreting the measured ILSR spectra.

The calculated spectra were obtained following initial geometry optimizations of the conformers of PEA molecules and of PEA-H_2O clusters, using the MMFF94s force field in Avogadro.[24] Then, these initial geometries were introduced in the GAUSSIAN 09 package[25] and optimized using "tight" self-consistent field convergence criteria and "ultrafine" integration grids. The optimization of the geometries of the conformers was performed by the Becke three parameter hybrid functional combined with Lee-Yang-Parr correlation functional (B3LYP)[26,27] and the 6-311++G(d,p) basis set. These geometries were used for calculation of harmonic and anharmonic vibrational frequencies and of Raman activities at the same level of theory. In addition, single-point energy calculations for finding minimum energies were carried out by second order Møller-Plesset theory (MP2)[28] with the same basis set.

c) Comparison of the measured to the calculated spectra for finding the best fit

The Euclidean distances related to the frequencies and intensities of the spectra were evaluated, while manually choosing the peaks from the experimental and theoretical spectra. These sets were then used to construct four new vectors of wavenumbers and intensities, i.e., V_{exp}, I_{exp}, V_{theo} and I_{theo}, where $V_{exp,theo}$ were the measured and calculated peak wavenumbers and $I_{exp,theo}$ - the respective peak intensities. The experimental and theoretical peaks were then arranged in pairs according to the fitting rule of minimal Euclidian distance: $\omega_{exp,theo} = \sqrt{\left(V_{exp} - V_{theo}\right)^2 + \left(I_{exp} - I_{theo}\right)^2}$, where $\omega_{exp,theo}$ was the distance between an experimental peak and its matched calculated peak. The average of the distances for each correlated peak pair gave a fitting quality indicator.

3 Results and Discussion

a) Resonant two-photon ionization

Mass-selected one-color R2PI spectra of PEA (m/z = 121), CH_2NH_2-H_2O (m/z = 48) and of PEA-H_2O (m/z = 139) in the region of the $S_1 \leftarrow S_0$ transitions are shown in Fig. 1 panels (a), (b) and (c), respectively. It is clearly seen that the PEA spectrum shows the A - E dominant features, labeled according to Refs. 13 and 14, and the other spectra show only single features. Actually, the A - D features were attributed to the four conformers of PEA,[10,13,14,15,18] while peak E was suggested to be a result of PEA-H_2O cluster fragmentation.[13,14] This is supported by the appearance of a nearly coincident peak in the fragmentation channel, m/z = 48, corresponding to the hydrated portion of the ethylamino tail and resulting from C_α-C_β bond cleavage. As already suggested,[14] the observation of this fragment can be considered as an indication that the PEA-H_2O cluster consists of a water molecule fused to the terminal amino group of PEA. Observation of the fragments related to only one of the conformers of the PEA-H_2O cluster is in line with the results of Melandri *et al*.[19] When they used Ar as carrier gas, or even He, they could not find rotational transitions belonging to other conformers that could have relaxed in the jet. Thus the addition of a single water molecule to PEA is considered to be accompanied by the collapse of its four conformers into a single structure, with the ethylamino side chain in a conformation related to the most highly populated conformer of the PEA monomer (see below).

Furthermore, examination of the R2PI spectrum, corresponding to the mass channel of PEA-H_2O, Fig. 1(c), shows only a feature shifted to the red (relative to E), but none of the A - E bands. Hence, this feature is attributed to a photofragment, implying

that ionization of PEA water clusters does not afford observation of the parent ions. This agrees with previous results, which pointed out that any of the PEA water clusters, even with near-threshold ionization lose at least one water molecule[13,14] and this feature was identified to be a fragment resulting from the PEA-$(H_2O)_3$ parent.

This behavior, where only fragments resulting from the parent clusters could be observed in the R2PI spectra may be explained by the dynamics in the ionic states. For example, feature E, comes from the excitation of a PEA-H_2O cluster and not from ionization of the PEA monomer. Nevertheless, its intensity is comparable to peaks A-D [Fig. 1(a)] that are associated with the PEA monomers. Since normally the number of clusters is much smaller than the number of monomers in the molecular beam, the transition probability for excitation of the cluster itself must be large to account for the large signal. By assuming that the electronic factors in the transition probability are the same for PEA and PEA-H_2O, it follows that the Franck-Condon (FC) factors for the cluster must not be smaller than the FC factors for PEA, thus leading to preparation of the excited (ionic) state that evolves to fragments, preventing the observation of the parent ion.

b) Ionization-loss stimulated Raman spectra

Although we were not able to directly monitor the R2PI spectrum of the PEA-H_2O parent ion, we were interested in testing whether it would be possible to obtain information on the PEA-H_2O cluster by monitoring ILSR spectra of the photofragments. Therefore, the ILSR spectra of the most stable PEA monomer and of the PEA and CH_2NH_2-H_2O fragments were measured, while parking the exciting UV laser on the C

and E bands, Fig. 1(a), and on the band in Fig. 1(b), respectively. Figure 2(a) shows the ILSR measured spectrum of the PEA fragment, and at the top of Figs. 3(a) and 3(b) and in Fig. 3(c), the ILSR measured spectra of the PEA monomer and of the PEA and CH_2NH_2-H_2O fragments, respectively, appear. These measured spectra, consist of sharp *Q*-branches of the transitions to different vibrational modes. Figure 2 also includes the calculated Raman spectra, the electronic ground state, S_0, structures, as well as the zero-point energy corrected electronic energies, evaluated by MP2/6-311++G(d,p) single point calculations with zero-point vibrational energy corrections from B3LYP/6-311++G(d,p)] levels of theory, of the gauche and anti conformers of the PEA-H_2O clusters, i.e., PEA(GI)-W, PEA(GIII)-W, PEA(GII)-W, PEA(AI)-W and PEA(AII)-W,[19] in panels (b), (c), (d), (e) and (f), respectively. The calculated Raman spectra are based on anharmonic vibrational frequencies and Raman intensities at the B3LYP/6-311++G(d,p) level of theory and they correspond to the electronic ground state, S_0, structures of the conformers of PEA-H_2O.

c) Determination of the structure corresponding to the measured ILSR spectrum of the PEA photofragment

By comparing the measured ILSR spectrum of the PEA fragment in Fig. 2(a), reflecting the PEA-H_2O cluster (see below), to the calculated Raman spectra of the PEA(GI)-W, PEA(GIII)-W, PEA(GII)-W, PEA(AI)-W and PEA(AII)-W conformers, Figs. 2(b) to 2(f), respectively, it can be determined which of the calculated Raman spectra resembles mostly the measured one. It is clearly seen that by visually comparing the measured ILSR spectrum, Fig. 2(a), and the calculated Raman spectra, the best

correspondence is obtained to the Raman spectrum related to the most stable gauche conformer PEA(GI)-W, shown in Fig. 2(b).

Furthermore, in the second step, fitting quality indicators, based on the Euclidian distances were calculated. For the conformers PEA(GI)-W, PEA(GIII)-W, PEA(GII)-W, PEA(AI)-W and PEA(AII)-W the indicators were found to be 8.07, 11.9, 10.7, 11.6 and 13.4, respectively. Since a lower distance, means greater similarity between the measured and a specific calculated spectrum, it is seen that the spectrum corresponding to the PEA(GI)-W structure best fits the measured spectrum, significantly better than the spectra of the other conformers. This implies that the measured ILSR spectrum of the PEA fragment corresponds to the most stable conformer, where the amino hydrogen of the side chain weakly interacts with the aromatic π cloud. This conformation is related to the most highly populated conformer of the PEA monomer with the H_2O HB directed to the nitrogen lone pair.

d) The PEA monomer and the PEA photofragment

Figures 3(a) and 3(b) include, at the bottom of the panels, the calculated Raman spectra, corresponding to the electronic ground state, S_0, structures of the most stable gauche conformers of PEA,[18] and of PEA-H_2O, namely PEA(GI)-W, following the above mentioned structure identification. In fact, the measured ILSR spectra indicate that the application of the SRS beams, i.e., ω_P and tunable ω_S, prior to the UV beam, which is parked on transitions corresponding to the PEA conformer, or to the PEA and CH_2NH_2-H_2O photofragments in the R2PI spectra allows excitation of vibrational transitions, whenever the frequency differences, ω_P - ω_S, match vibrational frequencies with high

enough Raman activities. These SRS transitions reduce the population of PEA molecules, or of PEA-H_2O clusters in the vibrational ground state, decreasing the number of ions and thus allowing generation of the measured ILSR spectra.

Comparison of the measured photofragment ILSR spectra of PEA [Fig. 3(b)] and of CH_2NH_2-H_2O [Fig. 3(c)] shows that they resemble very much, although the signal to noise ratio in the latter is poorer. On the other hand, some differences between the ILSR spectra of the PEA molecule [Fig. 3(a)] and of the photofragments [Figs. 3(b)] and 3(c)] are observed. These are related to some modes that appear only in a specific spectrum, belonging to one of the species, while others that seem to be only slightly perturbed and thus only somewhat shifted in frequencies (see Table S1 of the ESI).†

The most pronounced difference is the appearance of two new clear features in the high frequency range of the ILSR spectrum of the PEA photofragment, at 3717 and 3329 cm^{-1}, characterized by full width half maxima (FWHM) of 2.2 and 10 cm^{-1}, respectively. These two features are related to the fundamental O-H stretches of the unbound and bound water OH groups, respectively, and are close to the values observed by fluorescence-dip infrared spectroscopy in the tryptamine-H_2O cluster, 3716 and 3340 cm^{-1}.[29]

Comparison of the structures in Figs. 3(a) and 3(b), shows that the addition of water does not perturb the original conformation of the PEA monomer, but rather the PEA is approached by the water molecule with the hydrogen atom aiming toward the lone electron pair of the nitrogen atom. It is interesting to note that the structure of PEA-H_2O is completely different from that obtained very recently for the hydrated cluster of protonated PEA, i.e., H^+PEA-H_2O, due to the large variation in charge distributions.[30] In

this case, the infrared photodissociation (IRPD) spectra suggested two classes of isomers, whereas in the first one the H_2O was inserted into the NH^+-π bond of bare H^+PEA and was stabilized by two intermolecular NH^+-O and OH-π interactions, while in the slightly less stable second class of isomers the H_2O ligand acted as a an acceptor in a NH^+-O HB to one of the free NH bonds of the NH_3^+ group.

In the formed PEA-H_2O complex, the OH group of water can be considered as a HB donor[31] to the lone pair of nitrogen. The formation of the HB causes linewidth broadening of this feature and a large red shift (~ 325 cm^{-1}) of the stretching mode of the bound OH, relative to that of the H_2O monomer.[32] The large shift toward lower wavenumber, indicates a strong interaction upon HB formation, leading to weakening of the O-H covalent bond and therefore to a force constant of O-H···N considerable smaller than that of the non-bonded O-H. The strength of this HB is also supported by the calculated binding energy, obtained at the MP2/6-311++G(d,p) level of theory [with zero-point vibrational energy corrections from B3LYP/6-311++G(d,p)] of 2728 cm^{-1} and that estimated by the basis set superposition error (BSSE) correction via counterpoise correction,[33,34] which was found to be 2885 cm^{-1}.

Moreover, comparison of the calculation results, shown in Fig. 3(a) and 3(b), confirms the appearance of these two bands upon complexation of PEA with water, showing fairly good agreement with the observed spectra and indicating that the high frequency peak corresponds to the non-bonded fundamental O-H stretch, while the low one is that of the bound O-H stretch. Even more so, the large red shift of the bound O-H stretch pushed it beyond the N-H stretching region, being definitely consistent with the calculated Raman spectrum of the cluster.

As for the N-H stretching modes of PEA at 3414 and 3346 cm^{-1} and the C-H stretching modes of the ring and of the ethylamino group, above and below 3000 cm^{-1}, respectively, it can be clearly seen that they undergo only a little or no shift in wavenumber when the cluster is formed, agreeing quite well with the calculated values. Similar behavior is also observed in the lower frequency range that includes bending modes of the PEA and of the water as well as cooperative modes of the former. This is since the vibration modes of PEA-H_2O appear close to the corresponding PEA modes, or they are shifted to positions of other bands.

Nevertheless, when an expanded portion of the measured ILSRS spectra of PEA and of the PEA photofragment is shown in Figs. 4(a) and 4(b), respectively, it can be clearly seen that some differences occur. For example in the region below 1210 and around 880 cm^{-1} different patterns are observed in the spectra of the two species. Furthermore, the band at ~ 761 cm^{-1} is clearly seen in the measured ILSR spectrum of PEA, but missing in that of the PEA photofragment ILSR spectrum. This behavior is also observed in the calculated spectra and it turns out that this vibrational mode, corresponding to NH_2 wagging, is strongly hindered by the presence of the water molecule in the cluster.

It is important to note that although photofragment ILSR spectroscopy was used, the measured spectra of the PEA and CH_2NH_2-H_2O fragments are actually reminiscent of the signature of PEA-H_2O cluster. This could be understood by considering that the SRS vibrational excitation, which depleted some of the population of the ground vibrational states occurred prior to the UV excitation that fragmented the parent ion, thus allowing monitoring of the characteristic spectrum of the PEA-H_2O cluster.

4 Summary

The use of photofragment ILSRS together with DFT calculations allowed studying the most stable PEA-H_2O cluster in the gas phase. As shown, this method provides the opportunity to measure the characteristic ILSR spectral signatures of clusters that their parent ions could not be directly observed by R2PI, due to the fragmentation occurring in the ionic state. It is anticipated that this technique can be used for measurement of the spectra of photofragments resulting from other molecules or clusters and to allow their structural assignment.

Comparison of the spectra of PEA and of PEA-H_2O photofragments with the corresponding calculated spectra and particularly the analysis of the features representing the O-H stretch and other modes in the low frequency range showed that the lowest energy conformation of PEA in its water cluster is similar to bare PEA. This structure is characterized by an ethylamino tail, folded in a gauche arrangement, with the amino hydrogen weakly interacting with the aromatic π cloud and with the hydrogen of H_2O, pointing toward the nitrogen lone pair and forming a strong HB. The addition of the water molecule does not affect too much the PEA structure and even the flexible tail remains basically unaltered.

ACKNOWLEDGMENTS

We thank Otto Dopfer (Technical University of Berlin) for fruitful discussions. Financial support of this research by the German-Israeli Foundation for Scientific Research and Development (G.I.F) under Grant No. 1164-158.5/2011 and by the Israel Science Foundation (ISF) founded by The Israel Academy of Science and Humanities is gratefully acknowledged.

References

(1) J. P. Simons, *C. R. Chimie*, 2003, **6**, 17–31.

(2) J. P. Schermann, *Spectroscopy and Modeling of Biomolecules*; Elsevier: Amsterdam, The Netherlands, 2008.

(3) E. G. Robertson and J. P. Simons, *Phys. Chem. Chem. Phys*., 2001, **3**, 1-18.

(4) J. P. Simons, *Mol. Phys*., 2009, 107, 2435--2458.

(5) T. Ebata, A. Fujii, and N. Mikami, *Int. Rev. Phys. Chem.,* 1998, **17**, 331.

(6) T. S. Zwier, *J. Phys. Chem*. A 2001, **105**, 8827-.

(7) R. Weinkauf, J.P. Schermann, M. S. de Vries, and K. Kleinermanns, *Eur. Phys. J.* D, 2002, **20**, 309–316.

(8) M. S. de Vries and P. Hobza, *Ann. Rev. Phys. Chem*., 2007, **58**, 585-612.

(9) M. Mons, I. Dimicoli, and F. Piuzzi, *Int. Rev. Phys. Chem.*, 2002, ***21,*** 101-135.

(10) S.J. Martinez III, J.C. Alfano, and D.H. Levy, *J. Mol. Spectrosc.,* 1993, **158**, 82-92.

(11) S. Sun and E.R. Bernstein, *J. Am. Chem. Soc*., 1996, **118**, 5086-5095.

(12) J.Yao, H.S. Im, M. Foltin, and E.R .Bernstein, *J. Phys. Chem*. *A*, 2000, **104**, 6197-6211.

(13) J.A. Dickinson, M.R. Hockridge, R.T. Kroemer, E.G. Robertson, J.P. Simons, J. McCombie, and M. Walter, *J. Am. Chem. Soc*., 1998, **120**, 2622-2632.

(14) M.R. Hockridge and E.G. Robertson, *J. Phys. Chem. A*, 1999, **103**, 3618-3628.

(15) R. Weinkauf, F. Lehrer, E.W. Schlag, and A. Metsala, *Faraday Discuss*. 2000, **115**, 363-381.

(16) P.D. Godfrey, L.D. Hatherley, and R.D. Brown, J. Am. Chem. Soc., 1995, **117**, 8204-8210.

(17) J.C. López, V. Cortijo, S. Blanco, and J.L. Alonso, *Phys. Chem. Chem. Phys.,* 2007, **9**, 4521-4527.

(18) A. Golan, N. Mayorkas, S. Rosenwaks, and I. Bar, *J. Chem. Phys*., 2009, **131**, 024305.

(19) S. Melandri, A. Maris, B. M. Giuliano, L. B. Favero, and W. Caminati, *Phys. Chem. Chem. Phys*., 2010, **12**, 10210–10214.

(20) G. V. Hartland, B. F. Henson, V. A. Venturo, R. Hertz, and P. M. Felker, *J. Opt. Soc. Am. B*, 1990, **7**, 1950-1959.

(21) N. Mayorkas, I. Malka, and I. Bar, *Phys. Chem. Chem. Phys*., 2011, **13**, 6808–6815

(22) N. Mayorkas, S. Izbitski, A. Bernat, and I. Bar, *J. Phys. Chem. Lett*. 2012, **3**, 603−607; N. Mayorkas, A. Bernat, S. Izbitski, and I. Bar, *J. Chem. Phys*. 2013, **138**, 124312.

(23) M. Epshtein, A. Portnov, R. Kupfer, S. Rosenwaks, and I. Bar, *J. Chem. Phys.* 2013, **139**, 184201.

(24) Avogadro: an open-source molecular builder and visualization tool,

Version 1.00, see http://avogadro.openmolecules.net/; M. D. Hanwell, D. E. Curtis, D. C. Lonie, T. Vandermeersch, E. Zurek, G. R. J. Hutchison, *Cheminform*. **2012,** *4*, 17.

(25) M. J. Frisch, G. W. Trucks, H. B. Schlegel, G. E. Scuseria, M . A. Robb, J. R. Cheeseman, G. Scalmani, V. Barone, B. Mennucci, G. A. Petersson, H. Nakatsuji, M. Caricato, X. Li, H. P. Hratchian, A. F. Izmaylov, J. Bloino, G. Zheng, J. L. Sonnenberg, M. Hada, M. Ehara, K. Toyota, R. Fukuda, J. Hasegawa, M. Ishida, T. Nakajima, Y. Honda, O. Kitao, H . Nakai, T. Vreven, J. A. Montgomery Jr, J. E. Peralta, F. Ogliaro, M.Bearpark, J. J. Heyd, E. Brothers, K.N. Kudin,V. N. Staroverov, R. Kobayashi, J. Normand, K. Raghavachari, A. Rendell, J. C. Burant, S. S. Iyengar, J. Tomasi, M. Cossi, N. Rega, J. M. Millam, M. Klene, J. E. Knox, J. B. Cross,V. Bakken, C. Adamo, J. Jaramillo, R. Gomperts, R.E. Stratmann, O.Yazyev, A.J. Austin, R. Cammi,C. Pomelli, J. W. Ochterski, R. L. Martin, K. Morokuma, V. G. Zakrzewski, G. A. Voth, P. Salvador, J. J. Dannenberg, S. Dapprich, A. D. Daniels, Ö. Farkas, J. B. Foresman, J. V. Ortiz, J. Cioslowski, and D. J. Fox, Gaussian 09, revision C.01; Gaussian, Inc.: Wallingford, CT, 2010.

(26) A. D. Becke, *Phys. Rev. A*, 1988, **38**, 3098-3100.

(27) C. Lee, W. Yang, and R. G. Parr, *Phys. Rev. B*, 1988, **37**, 785-789.

(28) Chr. Møller and M. S. Plesset, *Phys. Rev*., 1934**, 46**, 618-622.

(29) J. R. Clarkson, J. M. Herbert, and T. S. Zwier,. *J. Chem. Phys*. 2007, **126**, 134306.

(30) A.Bouchet, M.Schütz, and O. Dopfer, unpublished.

(31) S. Melandri, *Phys. Chem. Chem. Phys*. 2011, **13**, 13901–13911.

(32) M.E. Jacox, Vibrational and Electronic Energy Levels of Polyatomic Transient Molecules in *NIST Chemistry WebBook, NIST Standard Reference Database Number 69*, Eds. P.J. Linstrom and W.G. Mallard, National Institute of Standards and Technology, Gaithersburg MD, 20899, http://webbook.nist.gov.

(33) S. F. Boys and F. Bernardi, *Mol. Phys*., 1970, **19**, 553-566.

(34) S. Simon, M. Duran, and J. J. Dannenberg, *J. Chem. Phys.*, 1996, **105**, 11024-11031.

Figure Captions

Fig. 1. One-color mass-selected resonantly enhanced two photon ionization spectra of (a) 2-phenylethylamine (PEA) (m/z = 121), and of (b) CH_2NH_2-H_2O (m/z = 48) and (c) PEA-H_2O (m/z = 139) fragments in the $S_1 \leftarrow S_0$ origin region. The vertical dashed line indicates the position of the feature related to PEA and CH_2NH_2-H_2O fragments.

Fig. 2. (a) Ionization-loss stimulated Raman spectrum, obtained when the UV laser is parked on the feature E related to the 2-phenylethylamine (PEA) fragment in Fig. 1(a) and panels (b), (c), (d), (e) and (f) represent the theoretical spectra of the PEA-H_2O clusters, corresponding to the shown electronic ground state, S_0, structures of PEA(GI)-W, PEA(GIII)-W, PEA(GII)-W, PEA(AI)-W and PEA(AII)-W, respectively. The calculated spectra are based on calculated anharmonic vibrational frequencies and Raman intensities at the B3LYP level with a 6-311++G(d,p) basis set for the corresponding structures and convoluted with Lorentzian lines of full width half maximum of 0.5 cm^{-1}. In each panel the geometries and the zero-point energy corrected electronic energies of the PEA-W conformers, as evaluated by single point Møller-Plesset calculations with the 6-311++G(d,p) basis set are shown.

Fig. 3. Ionization-loss stimulated Raman spectra obtained when the UV laser is parked on the features C (a) and E (b) related to 2-phenylethylamine (PEA) in Fig. 1(a) and on the hydrated tail portion (c) in Fig. 1(b). At the bottom of panels (a) and (b) the theoretical spectra of PEA and of PEA-H_2O, respectively, are displayed, based on the calculated

anharmonic vibrational frequencies and Raman intensities at the B3LYP level with a 6-311++G(d,p) basis set for the corresponding structures and convoluted with Lorentzian lines of full width half maximum of 0.5 cm^{-1}. The calculated Raman spectra reflect the spectra corresponding to the electronic ground state, S_0, structures of the most stable gauche conformers of the PEA monomer and of the PEA-H_2O cluster, shown in panels (a) and (b), respectively.

Fig. 4. An expanded portion of the ionization-loss stimulated Raman spectra obtained when the UV laser is parked on the C (a) and E (b) features related to 2-phenylethylamine (PEA) in Fig. 1(a). Also shown at the bottom of panels (a) and (b) are the theoretical spectra of PEA and of PEA-H_2O, respectively, based on the calculated anharmonic vibrational frequencies and Raman intensities at the B3LYP level with a 6-311++G(d,p) basis set for the most stable conformers and convoluted with Lorentzian lines of full width half maximum of 0.5 cm^{-1}. The black trace in panel (b) shows a zoomed portion of the spectrum.

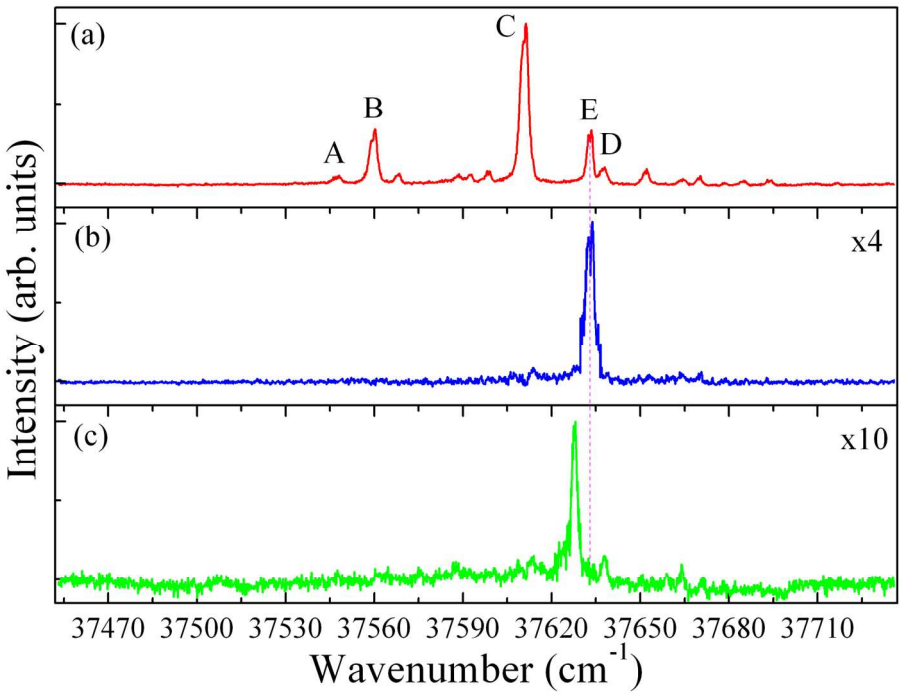

Mayorkas *et al*. RSCAdv. Fig. 1

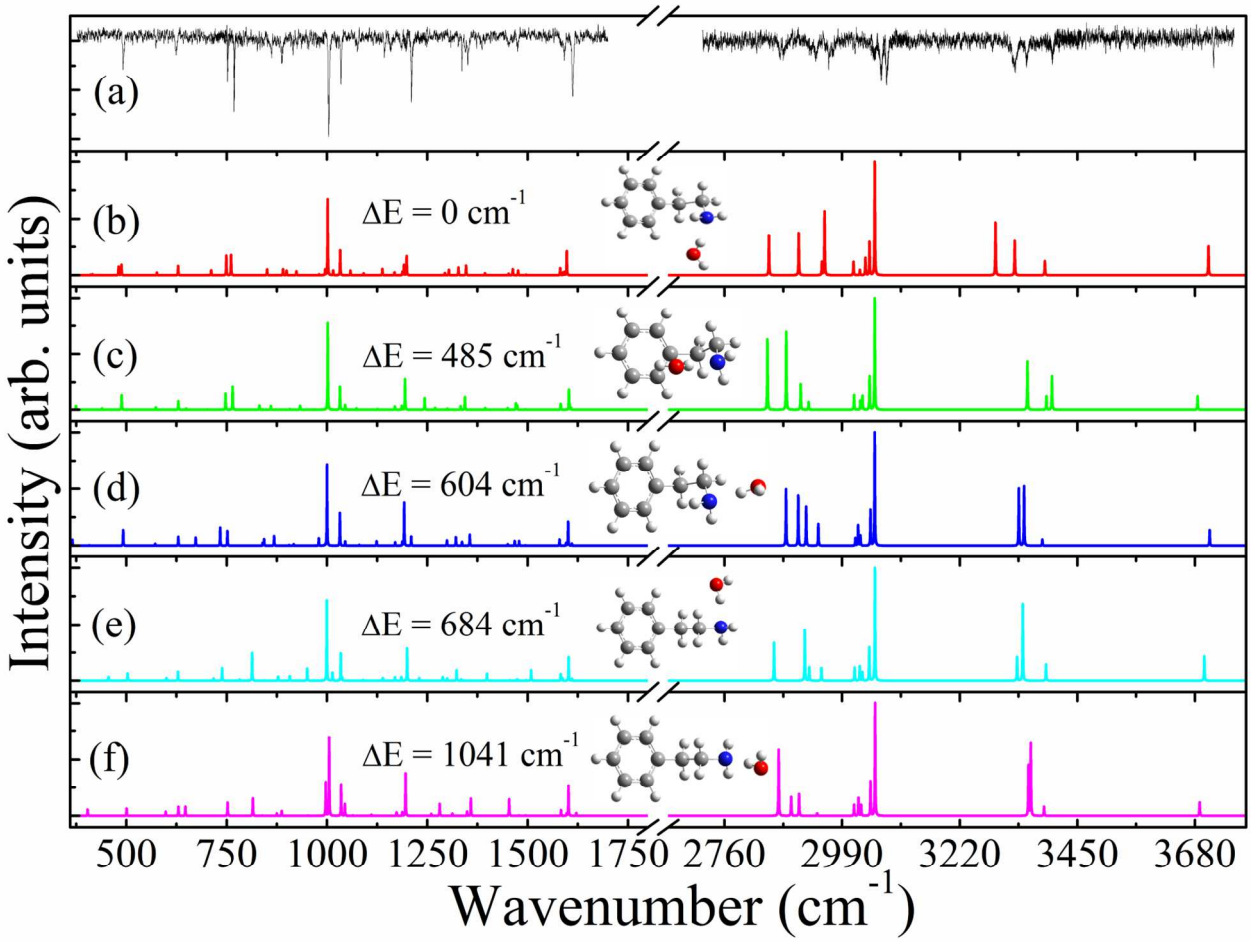

Mayorkas *et al*. RSCAdv. Fig. 2

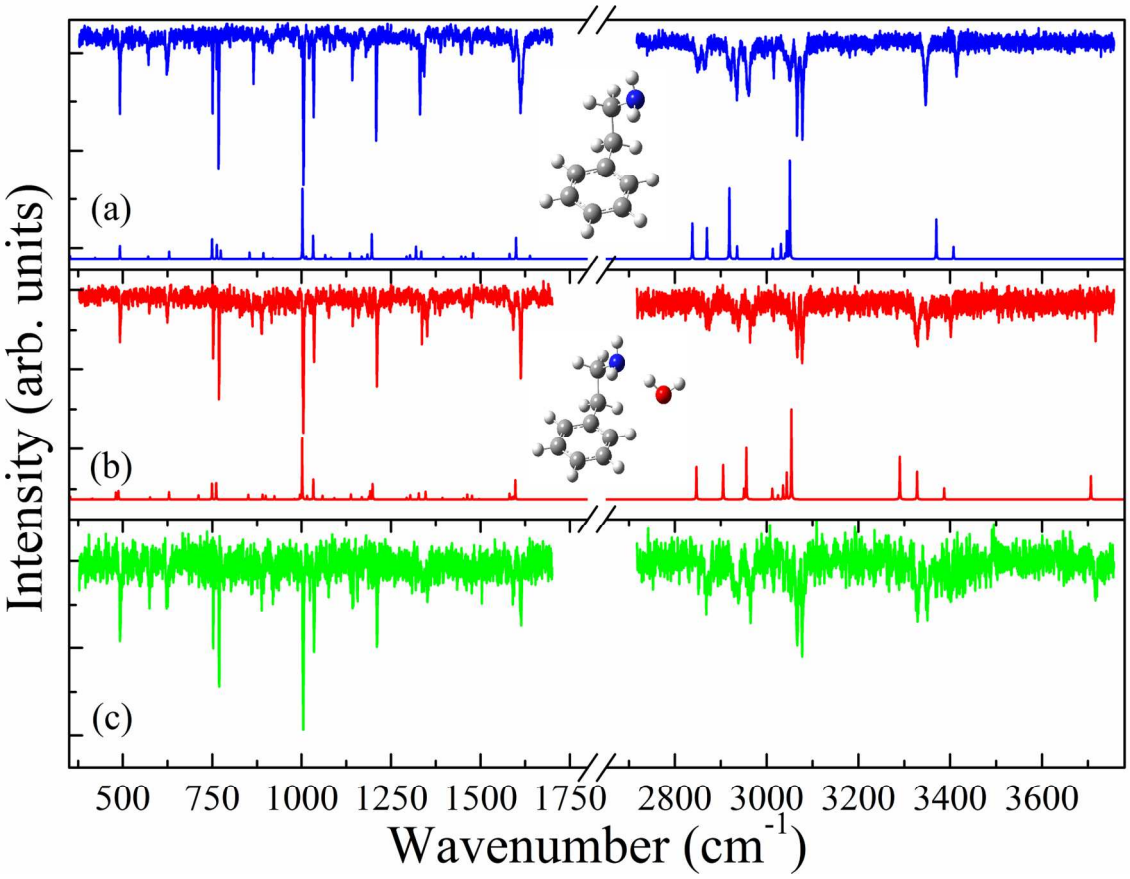

Mayorkas *et al*. RSCAdv. Fig. 3

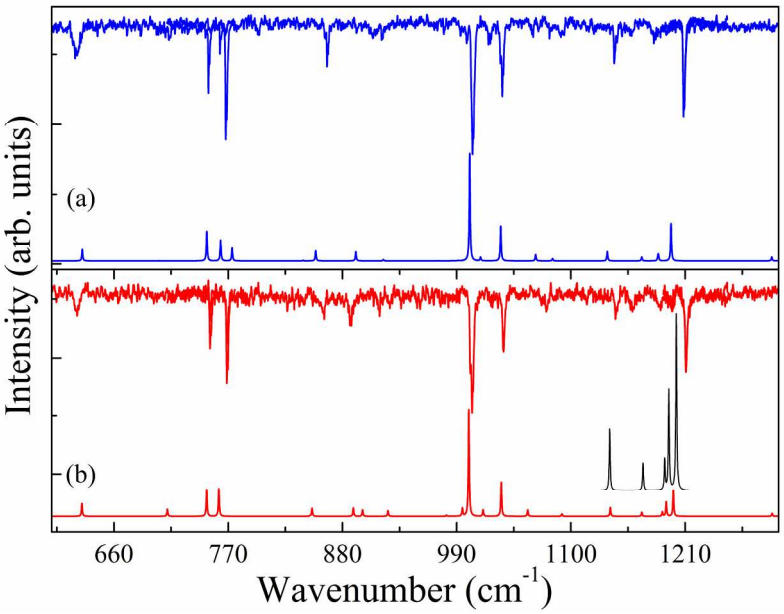

Mayorkas *et al*. RSCAdv. Fig. 4

Photofragment Ionization-loss Stimulated Raman Spectroscopy of a Hydrated Neurotransmitter: 2-Phenylethylamine–water

Nitzan Mayorkas, Snir Cohen, Hanan Sachs and Ilana Bar

The first use of photofragment ionization-loss stimulated Raman spectroscopy, in a broad range, for structural studies of clusters is reported.

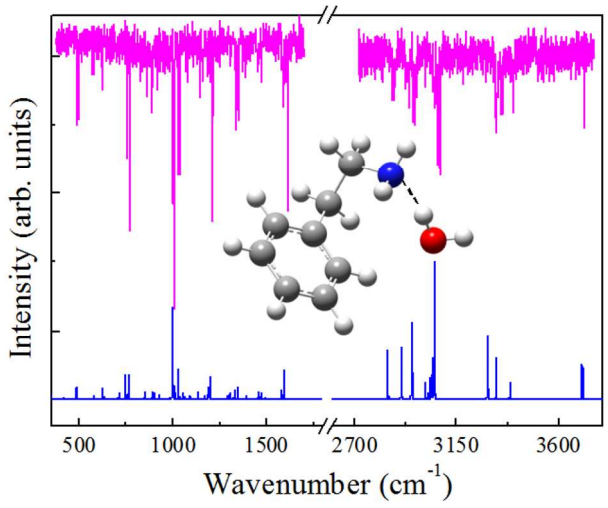

Mayorkas *et al*. RSCAdv. Table of contents entry